ELSEVIER

Journal of Photochemistry and Photobiology A: Chemistry 128 (1999) 57–63

Journal of Photochemistry and Photobiology A:Chemistry

www.elsevier.nl/locate/jphotochem

Sensitized electron transfer photooxygenation of acenaphthylene via competing sequential processes

Zhi-Qin Jiang [a,*], Ji-Feng Liu [a,1], Shu-Ping Wu [a], Qun Yu [b], Jian-Ping Ye [b]

[a] *Department of Chemistry, Tongji University, Shanghai 200092, PR China*

[b] *The Laboratory of Photochemistry, The Institute of Photographic Chemistry, Chinese Academy of Science, Beijing 100101, PR China*

Received 3 May 1999; received in revised form 21 June 1999; accepted 23 June 1999

Abstract

Photooxygenation of acenaphthylene (AN) sensitized by cyano-anthracenes was carried out in acetonitrile. The reaction leads to the initially-formed three precursors including acenaphthenone (ANO), acenaphthenequinone (AQ) and *cis*-dimer of AN (*c*-DAN). Each precursor undergoes a distinct sequential photooxygenation process, affording a series of carbonyl-containing products. The studies including product distribution, solvent-dependence, enhancement effect of biphenyl and fluorescence quenching etc. indicate that the title reactions proceed via a parallel three-sequence process in which the main pathways involve electron transfer mechanism.

Keywords: Acenaphthylene; Photoxygenation; Electron transfer; Competing sequence

1. Introduction

The electron transfer (ET) photooxygenations of electron-rich aromatic compounds initiated by electron-deficient cyanoaromatics have received increasing attention in recent years [1–3]. The fused aromatic hydrocarbons are known to react usually with singlet oxygen ($^1O_2$) [4], whereas their ET types of photooxygenations were less studied. Tokumaru et al. found that the CCT (contact charge transfer) photooxygenations of multi-methyl naphthalenes (Me_nN, $n=2$, 4) led to the endoperoxide formation by 1,4-cycloaddtion of the aromatic ring with $^1O_2$ [5]. Santamaria reported that the photooxygenation of 1,4-dimethylnaphthalene sensitized by 9,10-dicyanoanthracene (DCA) proceeded via competition between ET and $^1O_2$ pathway [6]. However, Takeshita reported that the dye-sensitized photooxygenation of acenaphthylene (AN) in methanol gave rise to the $^1O_2$-derived products including *cis*/*trans*-1, 2-diols and the corresponding 1/2-methoxy derivatives [7]. In this work, photooxygenation of AN in the presence of DCA or 9-cyanoanthracene (CNA) was further explored. It was found that AN undergoes a facile DCA- or CNA-sensitized photooxygenation in acetonitrile, furnishing entirely different carbonyl-containing products such as the 1-monoketone, 1,2-diketone (quinone), hydroxylactone and 1,2 -anhydride of AN. Both chemical and spectrometric studies reveal that the title reaction proceeds via a parallel-sequence process in which main pathways involve the electron transfer mechanism.

2. Experimental details

2.1. Reagents

DCA and CNA (Aldrich chemicals) were recrystallized from toluene, respectively. Biphenyl (BP) was recrystallized from alcohol, m.p. 69–71°C. Acenaphthylene (Fluka) was purified by repeated treatment of AN-picric acid complex according to the literature [8], m.p. 90–91°C (ref. 92–93°C). Acenaphthenone was obtained by a selective oxidation of acenaphthene with CrO_3 [9,10]. The crude product was recrystallized from benzene/ cyclohexane, m.p. 119–120°C (ref. 121.0–121.5°C). IR ν_{max} (KBr): 1712 (s, C=O) cm^{-1}; ^1H NMR $\delta(CDCl_3)$: 3.77 (2H, s), 7.47–8.10 (6H, m); MS (*m*/*e*): 168 (M^+). Acenaphthenequinone (AQ) was prepared in accordance with [11] and was recrystallized from toluene to give a yellow needle crystal, m.p.

* Corresponding author.

[1] Present address: Department of Chemistry, Massachusetts Institute of Technology, Cambridge, MA 02139, USA.

1010-6030/99/$ – see front matter
PII: S1010-6030(99)00137-9

Table 1
Sensitized photooxygenation of AN and product distributions

Entry no.	Substrate	Sensitizer/solvent	Irradiated time (h)	Conversion (%)	Product ratio (%)					
					ANO	AQ	**1**	**2**	**3**	*c*-DAN
1	AN	None/MeCN	10	5.1					10	82
2	AN	DCA/C_6H_6	12	7.5						90
3	AN	DCA/MeCN	2	17	18	7			50	16
4	AN	DCA/MeCN	8	98	5	3	17	15	50	
5	AN	CNA/MeCN	25	97	3	2	18	16	50	
6	ANO	DCA/MeCN	20	95			5	35	55	
7	ANO	DCA/BP/MeCN	9	94			8	32	55	
8	AQ	DCA/MeCN	5	95				83		
9	AQ	None/MeCN	3	94				82		
10	1	DCA/MeCN	12	96				32	50	
11	*c*-DAN	DCA/MeCN	12	90	2		15	10	46	

259–260°C. MS (*m*/*e*): 182 (M^+), 154 (M^+–CO, 100%). 1,8-(3′-hydroxy)-*δ*-naphthalene lactone **1** was prepared according to the literature method [12], recrystallized from xylene, m.p. 167–169°C (ref. 169–171°C). IR ν_{max} (KBr): 3276 (s, OH), 1680 (s, C=O) cm^{-1}; ^1H NMR $\delta(CDCl_3)$: 6.92 (s, 1H), 7.60–7.72 (m, 3H), 7.97 (d, 1H, $J = 8.1$ Hz), 8.16 (d, 1H, $J = 8.1$ Hz), 8.44 (d, 1H, $J = 6.9$ Hz); MS (*m*/*z*): 200 (M^+), 155 (100%). *Cis*-dimer of acenaphthylene (*c*-DAN) was obtained by photo-dimerization of AN under oxygen atmosphere in hexane. The crude product was recrystallized from hexane/benzene, m.p. 230–232°C (231–233.5°C [13]). Solvents for photolysis and spectrometric experiments were purified and distilled before use.

2.2. Instruments

Shimadzu UV-240, Nicolet FT-5DX IR, Perkin–Elmer LS-50 fluorophotometer, Bruker AM-400 NMR and Finnigan 4021 GC-MS spectrometers were employed in this work. The transient fluorescence decay and lifetime were detected on Horiba NAES-1100 single-photon counting transient fluorophotometer. Redox potentials were measured on HPD-1A cyclic voltammogram instrument by using Pt–Pt–SCE three-electrode system. Shimadru-9A gas chromatograph was used with packed column (SE-30, 10%) and flame ionization detector. Quantum yields for the consumption of AN or ANO were measured using potassium ferrioxalate actinometry, in which conversions of the substrates were controlled to about 10%.

2.3. Photooxygenation procedures

DCA- and CNA-sensitized photolysis experiments of entry 1–11 (Table 1) were carried out in a Pyrex-glass reactor attached with a water-cooled jacket. Light source was a 500 W medium-pressure mercury lamp with an automatic controller. The tested sample solution in a Pyrex-glass tube was irradiated with continuous oxygen bubbling. The reaction progress was monitored by TLC and the irradiated samples were analyzed by GC (SE-30, 10%, benzil as internal standard) to determine the conversion of AN and the product ratios of ANO, AQ and **1**–**2**. In addition, preparative scale of irradiated samples were chromatographed on silica-gel column with an initial elution of cyclohexane-ethyl acetate to isolate *c*-DAN, the recovered AN and products (ANO, AQ, **1**–**2**), then with a final elution of methanol to obtain the oxidized oligomer **3** ($m/e \geq 1000$). The identifications of these isolated compounds were made by conventional spectrometry methods (IR, NMR and MS) and compared with the authentic compounds prepared according to the literature as described in Section 2.1. The amounts of *c*-DAN and **3** based on silica-gel chromatograph isolation were further taken into determination of the overall product ratios. The data for the experiment entry 1–11 are listed in Table 1.

3. Results and discussion

3.1. Sensitized photooxygenation of AN and stepwise pattern

The photooxygenations of AN (4×10^{-2} mol dm^{-3}) sensitized by DCA or CNA (4×10^{-4} mol dm^{-3}) were carried out in acetonitrile. The reactions completed in 8–25 h and afforded merely the carbonyl-containing derivatives of AN such as acenaphthenone (ANO), 1,2-acenaphthenequinone (AQ), 1,8-(3′-hydroxy)-*δ*-naphthalene lactone **1**, and 1,8-naphthalene dicarboxylic anhydride **2** along with an oxidized oligomer **3** ($m/e \geq 1000$) as shown in Scheme 1 and entry 4, 5 in Table 1. However, no photooxygenation but dimerization of AN were observed when the experiment was performed in benzene (entry 1, see later discussion). This implies that the title reaction may involve ET processes.

It can be seen that the products are entirely different as compared to the reported $^1O_2$-derived reaction of AN in methanol sensitized by rose bengal (RB) in which the products were *cis*/*trans*-1,2-dihydroxyacenaphthene and their

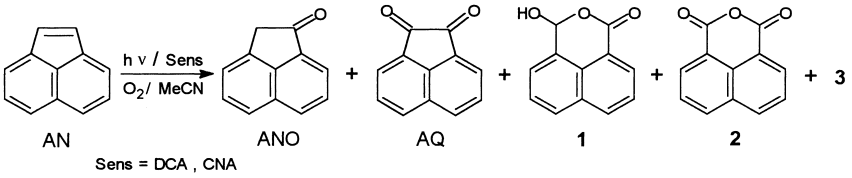

Scheme 1.

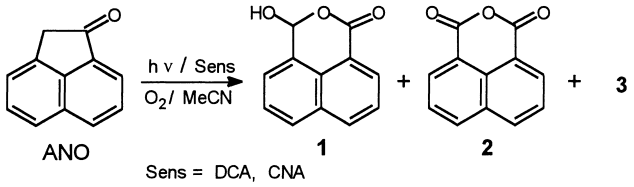

Scheme 2.

mono-methyl ethers [7]. Besides, the reported $^1O_2$ reaction of AN proceeds much slower than the title reaction of this work.

In our recent work [14,15], it was demonstrated that the mono-ketone ANO underwent a facile DCA-sensitized photooxygenation (entry 6) to give the hydroxy-lactone **1**, anhydride **2** and oligomer **3**. Whereas the photooxygenation of **1** in turn gave rise easily to **2** and **3** under the same conditions (entry 10). In other words, both the control experiments indicated that the reaction takes place with a sequential manner, which can be referred as the first sequence : AN → ANO → **1** → **2**. Furthermore, the reaction of ANO was proved to undergo a PET pathway, in which ANO and **1** as electron donors react with the electron-accepting singlet ^{1}DCA (Scheme 2).

In order to examine further the whole product origins, more control tests were performed, in which the reactions were conducted to different stages by controlling the reaction conversions. The results are summarized in Table 1.

Interestingly, the results of entry 1 and 2 show that when irradiation on AN under oxygen atmosphere were carried out either in the absence of DCA in MeCN or in the presence of DCA in benzene, the major product was detected as the *cis*-dimer of AN (*c*-DAN). Both the reactions undertook much slower as compared with the DCA-sensitized photooxygenation of AN in MeCN (entry 4). These facts indicate that the photo-dimerization of AN occurs, leading to selective formation of *c*-DAN in those cases. No *trans*-dimer of AN (*t*-DAN) was found under the same conditions. This is consistent with the literature reports [8]. It was proved that oxygen can effectively quench the triplet AN that favors formation of *t*-DAN. Therefore, the singlet AN^1 is predominate to form the singlet excimer, $(AN–AN)^1$, which leads to the formation of *c*-DAN.

A further DCA-sensitized photooxygenation of the authentic *c*-DAN in MeCN was executed, resulting in the formations of ANO, **1** and **2**, in which **1** and **2** are the major products (see entry 11), no formation of AQ was observed. This novel finding indicates the existence of a second reaction sequence: AN → *c*-DAN → ANO → **1** → **2** in the title reaction.

Furthermore, the data in entry 3–5 indicate that a minor product AQ was produced during the reaction. Nevertheless, quinone AQ was not found in the controlled photooxygenations of either ANO or *c*-DAN sensitized by DCA in MeCN (see entry 6, 11). These imply that AQ is most likely to be generated directly from AN rather than from the precursors ANO and *c*-DAN. In addition, further photooxygenation of AQ in either present or absence of DCA (entry 8, 9) led to direct formation of the anhydride **2** without passing through the stage of **1**. Therefore, the third reaction sequence can be expressed as AN → AQ → **2**. Schuster also reported that AQ was readily oxidized to **2** by auto-oxidation in CH_2Cl_2 [16]. To verify this postulate, the title reaction was controlled to a lower conversion of AN, e.g. 17% (entry 3). The reaction gave the major products, *c*-DAN (16%) and ANO (18%), along with AQ (7%). Whereas, the yields of ANO and AQ decreased considerably at high conversion of AN, and *c*-DAN disappeared (entry 4, 5). All above results have elucidated that the simultaneous formations of the three precursors, monoketone ANO, quinone AQ and *c*-DAN, compete each other in the initial stage of the reaction. Each precursor undergoes a subsequent competing sequence photooxygenation. This parallel three-sequence process is summarized in Scheme 3.

By comparison of the above observations it can be seen that the sequence 1 is likely faster than the sequence 2 and 3, or in other words, the sequence 1 should dominate the title reaction.

3.2. Reaction mechanism

The above results also reveal that among the three sequence pathways, sequence 1, 2 and initial step of sequence 3 proceed via a possible ET mechanism since we found that AN, authentic ANO and *c*-DAN do not undergo their characteristic DCA-sensitized photooxygenation in non-polar solvent such as benzene, respectively.

3.2.1. Changes in free energy of PET

The driving force for the primary PET process of the substrates such as AN, ANO and *c*-DAN with the singlet ^{1}DCA can be predicted by the Rehm–Weller formula [17]

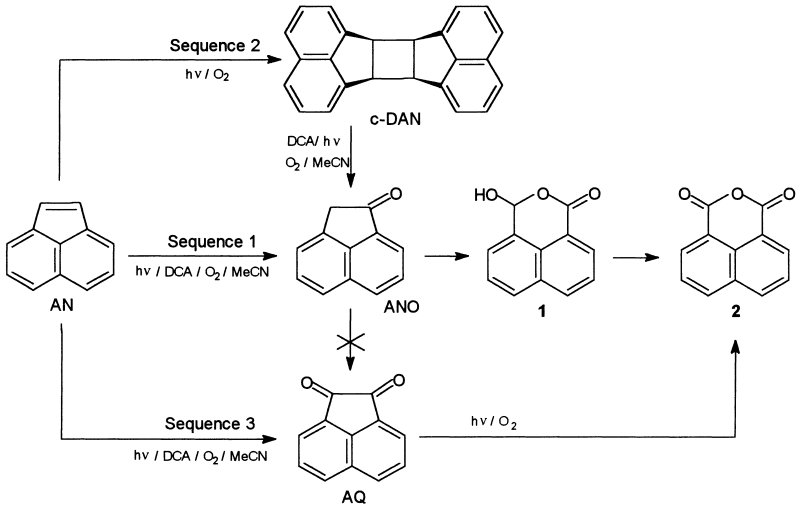

Scheme 3.

Table 2
Free energy change of PET processes of substrates and ^{1}DCA in MeCN

Substrate	E^{ox} V (vs. SCE)	ΔG_1 (kcal mol^{-1})	$k_q(s)$ ($\times 10^{-9}$ M^{-1} s^{-1})	$k_q(t)$ ($\times 10^{-9}$ M^{-1} s^{-1})
AN	1.62	−8.3	40.1	20.2
ANO	1.78	−4.7	11.7	10.5
c-DAN	1.89	−2.1	8.0	6.0

where the substrates (AN, ANO and *c*-DAN) act as electron donors (D) in their ground states.

$$\Delta G = \left[23.06E^{ox}(D) - E^{red}(A) - \frac{e_0^2}{\alpha\varepsilon} - E_{0,0} \right]$$

The data are listed in Table 2. The oxidation potentials, E^{ox}(D), of AN, ANO and *c*-DAN were measured in MeCN by cyclic voltammetry, being 1.62, 1.78 and 1.89 V versus SCE, respectively. The reduction potential (E^{red}) and singlet energy ($E_{0,0}$) of DCA are known to be −0.97 V and 2.89 eV, respectively, and the value of $e_0^2/\alpha\varepsilon$ in MeCN equals 0.06 [18]. The free energy change, ΔG_1, for the primary ET process from substrates (AN, ANO, *c*-DAN) to ^{1}DCA was calculated as −8.3, −4.7 and −2.1 kcal mol^{-1}, respectively, which imply that these PET processes are thermodynamically favored. ΔG_2 for the secondary ET of DCA$^{\bullet-}$.and O_2 to yield $O_2^{\bullet-}$ is estimated as −3.5 kcal mol^{-1} according to $E^{red}(O_2^{\bullet-}/O_2) = -0.82$ V. Combination of D$^{\bullet+}$ and $O_2^{\bullet-}$ leads to the oxidized product. Therefore, the title reactions could be proposed as follows:

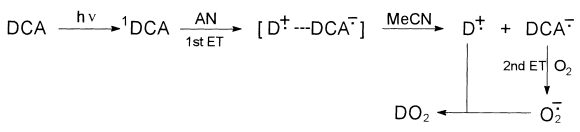

The driving force for each donor/acceptor pair lies in the order: AN/DCA > ANO/DCA > *c*-DAN/DCA. This prediction is in accordance with the preceding chemical evidence of the predominate sequence 1 (AN → ANO → **1** → **2**). It is unlikely that back electron transfer from $O_2^{\bullet-}$ to D$^{\bullet+}$ such as AN$^{\bullet+}$, ANO$^{\bullet+}$ to regenerate singlet oxygen because it was proved that rose bengal (a typical singlet oxygen sensitizer [4])-sensitized photooxygenation of AN gave only non-carbonyl products such as *cis*/*trans*-1,2-dihydroxyacenaphthene and their mono-methyl ethers [7], which are entirely different to the carbonyl type of products in our case (see entry 3,4 and 5 in Table 1). Besides, the reported $^1O_2$ reaction of AN proceeds much slower than the title reaction of this work. In Scheme 3, although AN → AQ is an ET process, the PET of quinone AQ with ^{1}DCA is not accessible due to the poor electron-donating ability of AQ in comparison with ANO or *c*-DAN. Therefore, subsequent oxidation of AQ to give **2** should not be ET-initiated reaction.

On the other hand, several studies have revealed that in PET processes for some aromatic substrates such as 1,1-diphenylethylene, the radical cation D$^{\bullet+}$ can react further with the ground D [2,3]. In our case, this competing pathway, if exists, might induce dimerization producing $D_2^{\bullet+}$ or even oligomerization to give $D_n^{\bullet+}$ and further oxygenation of $D_n^{\bullet+}$ with $O_2^{\bullet-}$ could lead to formation of the oligomer **3**.

Alternatively, for a number of electron-rich donors, D, particularly some aromatic hydrocarbons [3], facile deprotonation of D$^{\bullet+}$ takes place, leading to the formation of D$^{\bullet}$, due to highly negative pK_a of these radical cations. Thus, D$^{\bullet}$ can react with O_2 to give DOO$^{\bullet}$ and final products. However, this situation may not suit our case since pK_a of AN$^{\bullet+}$ could be estimated not high enough to undergo deprotonation.

3.2.2. Fluorescence quenching of DCA by substrates

The fluorescence quenching of DCA was studied using both static and transient quenching techniques. It was found that the fluorescence of DCA in MeCN was effectively quenched by AN, ANO, and *c*-DAN, respectively. The static and transient quenching rate constants $k_q(s)$ and $k_q(t)$ were determined by the Stern–Volmer plots according to the Eqs. (1) and (2),

$$\frac{\Phi_0}{\Phi} = 1 + k_q(s)\,[Q] \quad (1)$$

$$\frac{\tau_0}{\tau} = 1 + k_q(t)\,[Q] \quad (2)$$

herein Φ_0, Φ are the fluorescence quantum yields measured by the relative fluorescence intensity of DCA in the absence and presence of the quencher Q, respectively. τ_0/τ refers to the ratio of fluorescence lifetimes of DCA in the absence and presence of quencher. The Stern–Volmer plots show good linear correlation ($r \geq 0.990$). The data of $k_q(s)$ and $k_q(t)$ for the quenchers (AN, ANO, *c*-DAN) in Table 2 are close to an order of diffusion-controlled rate ($\sim 10^{10}\,M^{-1}\,s^{-1}$), which indicate that the quenching are characteristic of ET process. The interactions of the quenchers and DCA in their ground states are negligible because both values of $k_q(s)$ and $k_q(t)$ are close to each other.

3.2.3. Enhanced effect of BP on the photooxygenation

Some aromatics can behave as a relay via secondary ET to accelerate the desired ET process [19]. Accordingly, biphenyl (BP) was used as a co-sensitizer in the DCA-sensitized photooxygenation of AN and ANO, respectively. The enhanced action of BP on both photooxygenations of AN and ANO was observed. The results in Table 3 indicate that the quantum yields Φ_d for the disappearance of AN or ANO in DCA-sensitized photooxygenation increase substantially by 0.7 or 1.6 fold when BP was added to the AN/DCA ([BP]/[AN] = 0.5) or ANO/DCA ([BP]/[ANO] = 0.5) system, respectively. In addition, the data of entry 6 and 7 in Table 1 also show that the DCA-sensitized photooxygenation of ANO is considerably accelerated by adding BP. However, the product distribution (ratios) remains essentially unchanged in the absence and presence of BP. This implies that the reaction

Table 3
Enhanced effect of BP on DCA-sensitized photooxygenactions of AN and ANO[a]

[Substrate] (mol dm^{-3})	[BP] (mol dm^{-1})	(Φ_d)[b]
[AN] = 0.034	0	0.08
[AN] = 0.034	0.017	0.14
[ANO] = 0.030	0	0.05
[ANO] = 0.030	0.017	0.18

[a] [DCA] = 4×10^{-4} mol dm^{-3}.

[b] Φ_d is the consumed quantum yield, measured by potassium ferrioxalate actinomter at conversions of AN or ANO < 10%.

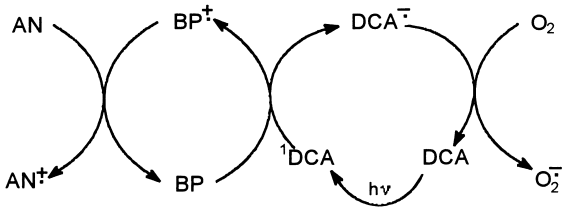

Scheme 4.

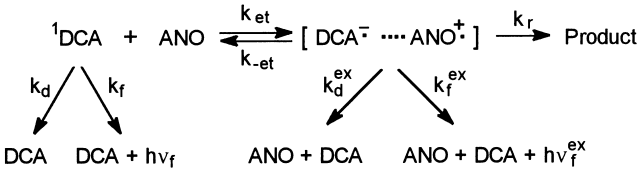

Scheme 5.

was enhanced apparently by adding BP but the nature of ET mechanism still remains the same in both cases. Formation of the radical cation, $BP^{\bullet+}$, in the primary ET from BP to ^{1}DCA is thermodynamically favored because of its negative ΔG (-2.8 kcal mol^{-1}). This process was proved as an efficient one by Farid et al. in a transient spectrometry study [19]. The secondary ET from AN or ANO to $BP^{\bullet+}$ gives rise to $AN^{\bullet+}$ or $ANO^{\bullet+}$ due to higher oxidation potential of BP (E^{OX} = 1.86 V) than AN and ANO (Table 2). Therefore, these ET lead to increase of both the concentrations of $ANO^{\bullet+}$ and $DCA^{\bullet-}$. This enhancement effect of BP corresponds to insert an efficient ET chain of BP in the original ANO/DCA ET cycle as depicted in Scheme 4.

3.2.4. Fluorescence kinetics of the exciplex ANO/DCA

Since ANO is proposed to be the principle precursor in the title reaction, the fluorescence quenching of DCA by ANO was further examined. Formation of the exciplex (DCA/ANO)* based on its weak emission at 470–520 nm in different solvents including hexane, cyclohexane, chloroform and acetonitrile was also observed. The exciplex emission, λ_{max}^{ex}, show an apparent red-shift upto 43 nm in acetonitrile than in hexane, whereas the emission intensity decreases with increase of the solvent polarity, indicating that charge separation of the radical-ion pair, $ANO^{\bullet+}/DCA^{\bullet-}$, depends on the solvent polarity [20]. In addition, existence of the radical-ion pair, $ANO^{\bullet+}/DCA^{\bullet-}$, was demonstrated by a CIDNP study [15].

It is well documented that formation and transformation of the exciplex play important role in the PET processes. The Ware model for the transient exciplex kinetics [21] was employed to estimate approximate rate constants involved in the DCA/ANO system as shown in Scheme 5.

The fluorescence decay curves of DCA (4×10^{-5} M) at 448 nm in cyclohexane with different concentrations of ANO in the time interval (0–100 ns) were found to be bi-exponential, whereas that at 530 nm are approximately mono-exponential. The bi-exponential decays can be

Table 4
Transient fluorescence decay of DCA with different [ANO] in cyclohexane

[ANO] 10^{-2} M	$\lambda = 448$ nm				$\lambda = 530$ nm	
	C_1	τ_1 (ns)	C_2	τ_2 (ns)	C	τ_{ex} (ns)
0.6	0.158	5.43	0.0587	13.1	0.188	14.5
1.2	0.172	5.07	0.0585	12.2	0.195	14.2
1.8	0.164	4.47	0.0224	14.9	0.172	14.0
2.4	0.170	3.44	0.0285	13.8	0.188	13.7
3.0	0.200	2.89	0.0315	13.5	0.167	13.5
3.6	0.217	2.59	0.0340	14.0	0.163	13.8

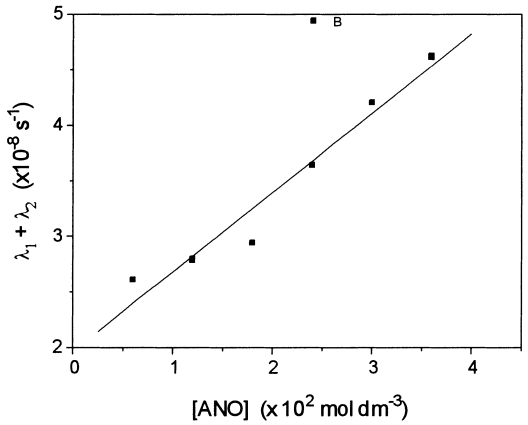

Fig. 1. Plot of $(\lambda_1 + \lambda_2)$ vs. [ANO] obtained From the fluorescence decays of DCA in cyclohexane.

expressed by the formula (3):

$$[^1\text{DCA}] = C_1 e^{\lambda_1 t} + C_2 e^{\lambda_2 t} \quad (3)$$

in which λ_1, λ_2 are the decay parameters related to the concentration of ANO, respectively, and $\lambda_1 + \lambda_2 = 1/\tau_1 + 1/\tau_2$. C_1 and C_2 are constants. The data are listed in Table 4. As seen from the preceding results of steady fluorescence quenching [15], the emission at 530 nm should be attributed to the exciplex fluorescence. Moreover, the data in Table 4 also indicates that τ_{ex} decreases slightly with the increase of [ANO] although the change is comparably small. The average values of τ_{ex} is 14.0 ± 0.5 ns. With the steady-state treatment, we can obtain

$$\lambda_1 + \lambda_2 = k_d + k_f + k_{-et} + k_p + k_{et}[\text{ANO}] \quad (4)$$

here $k_p = k_r + k_f^{ex} + k_d^{ex}$ and $\lambda_1 + \lambda_2$ should be a linear function of [ANO]. The deconvolution of the decay curve gives the values of $\lambda_1 + \lambda_2$. The plot of $(\lambda_1 + \lambda_2)$ vs. [ANO] shows a good linearity ($r = 0.976$, see Fig. 1). Hence the values of k_{et} and $(k_d + k_f + k_{-et} + k_p)$ can be calculated from the plot slope and intercept, respectively.

For the first-order process

$$k_d + k_f = \frac{1}{\tau_o} \quad \text{and} \quad k_d^{ex} + k_f^{ex} = \frac{1}{\tau_{ex}} \quad (5)$$

When the values of $k_q(s)$ and $k_q(t)$ are close to each other and reach to the diffusion-controlled limit, there is

$$K_q = \frac{k_{et} k_p}{(k_{-et} + k_p)} \quad (6)$$

Since the values of τ_o (10.9 ns) of ^{1}DCA and k_q (6.6×10^9 M^{-1} s^{-1}) were measured in cyclohexane, all the kinetic rates are estimated approximately from the Eqs. (4)–(6)and summarized in Table 5. It can be concluded that both values of k_{et} and k_q are diffusion-controlled and close to each other, which indicates that the exciplex formation by ET from ANO to ^{1}DCA is the predominate process in the fluorescence quenching. Furthermore, $k_{et} \gg k_{-et}$ and $k_{et} \gg k_d + k_f$, which mean that the forward ET (k_{et}) is much faster than the reverse ET (k_{-et}) by $\sim 8.8 \times 10^2$ folds and also than the deactivations through the non-radiation (back et) and radiation decay processes of the exciplex ($k_d^{ex} + k_f^{ex}$)approximately by ~ 100 folds.

4. Conclusion

Di- and mono-cyanoanthracene-sensitized photooxygenation of acenaphthylene in this work has been proved to undergo a competing sequential reaction. The reaction leads to three initially generated precursors (acenaphthenone, 1,2-acenaphthene-quinone and the *cis*-dimer of acenaphthylene). Each precursor undergoes distinct sequential photooxygenation, furnishing carbonyl-containing products.

The chemical, spectrometric and dynamic experiments have verified that the sequence 1 (AN → ANO → **1** → **2**) and 2 (AN → *c*-DAN → ANO → **1** → **2**) are essentially ET-derived processes. In sequence 3 (AN → AQ → **2**), the initial step (AN → AQ) is ET-controlled reaction, whereas the subsequent step (AQ → **2**) is not. Therefore, the title reaction is mainly PET process.

Acknowledgements

This work was supported by the National Natural Science Foundation of China (NNSFC, No. 29772025). We also extend thanks to the reviewer, Y. Jiang, from the Research Institute of Schering-Plough, USA, for his fruitful discussions and suggestions on the manuscript.

Table 5
Estimated kinetic parameters for the exciplex (ANO/DCA)* in cyclohexane

τ_o (ns)	τ_{ex} (ns)	k_q (M^{-1} s^{-1})	k_{et} (M^{-1} s^{-1})	k_{-et} (s^{-1})	$k_d^{ex} + k_f^{ex}$ (s^{-1})	$k_d + k_f$ (s^{-1})	k_r (s^{-1})
10.9	14.0	6.6×10^9	7.2×10^9	0.82×10^7	7.1×10^7	9.2×10^7	1.9×10^7

References

[1] M.A. Fox, M. Chanon, Photoinduced Electron Transfer, Part A–D, Elsevier, Amsterdam, 1988.
[2] N.J. Turro, Chem. Rev. 86 (1986) 401.
[3] Z.Q. Jiang, Res. Chem. Intermed. 14 (1990) 185.
[4] A.P. Schaap (Ed.), Singlet Molecular Oxygen, Halsted Press, New York, 1976
[5] K. Onodera, G.-L. Furusawa, M. Kojima, M. Tsuchiya, R. Akaba, H. Sakuragi, K. Tokumaru, Tetrahedron 41 (1985) 2215.
[6] T.B. Truong, J. Santamaria, J. Chem. Soc. Perkin Trans. 2 (1987) 1.
[7] T. Hatsui, H. Takeshita, Bull. Chem. Soc. Jpn. 53 (1980) 2655.
[8] D.O. Cowan, J.C. Kozier, J. Am. Chem. Soc. 97 (1975) 250.
[9] L.F. Fieser, J. Cason, J. Am. Chem. Soc. 62 (1940) 432.
[10] T. Urbansky, M. Wolff, Roczniki Chem. 39 (1965) 1447, Cf. C. A., 64 (1965) 17507f.
[11] E.C. Hornig, Org. Synthesis, Coll. 3 (1955) 1.
[12] H. Bader, Y.H. Chiang, Synthesis 4 (1976) 249.
[13] J.M. Nerbonne, R.G. Weiss, J. Am. Chem. Soc. 101 (1977) 402.
[14] Z.Q. Jiang, J.F. Liu, Acta Chimica Sinica (Eng. Ed.), (1988) 377.
[15] S.P. Wu, J.F. Liu, Z.Q. Jiang, J. Chem. Soc. Chem. Commun. (1996) 493.
[16] J.Y. Koo, G.B. Schuster, J. Org. Chem. 44 (1979) 847.
[17] D. Rehm, A. Weller, Israel J. Chem. 8 (1970) 259.
[18] C.S. Foote, J. Eriksen, J. Phys. Chem. 82 (1978) 2659.
[19] I.R. Gould, D. Ege, J.E. Moser, S. Farid, J. Am. Chem. Soc. 112 (1990) 4290.
[20] H. Masuhara, N. Mataga, Acc. Chem. Res. 14 (1981) 312.
[21] W.R. Ware, J.D. Holmes, D.R. Arnold, J. Am. Chem. Soc. 96 (1974) 7861.